

Thermodynamics and Phase Transition of a Nonlinear Electrodynamics Black Hole in a Cavity

Peng Wang,^{*} Houwen Wu,[†] and Haitang Yang[‡]

*Center for Theoretical Physics, College of Physical Science and Technology,
Sichuan University, Chengdu, 610064, China*

Abstract

We discuss the thermodynamics of a general nonlinear electrodynamics (NLED) asymptotically flat black hole enclosed in a finite spherical cavity. A canonical ensemble is considered, which means that the temperature and the charge on the wall of the cavity are fixed. After the free energy is obtained by computing the Euclidean action, it shows that the first law of thermodynamics is satisfied at the locally stationary points of the free energy. Focusing on a Born-Infeld (BI) black hole in a cavity, the phase structure and transition in various regions of the parameter space are investigated. In the region where the BI electrodynamics has weak nonlinearities, Hawking-Page-like and van der Waals-like phase transitions occur, and a tricritical point appears. In the region where the BI electrodynamics has strong enough nonlinearities, only Hawking-Page-like phase transitions occur. The phase diagram of the BI black hole in a cavity can have dissimilarity from that of a BI black hole using asymptotically anti-de Sitter boundary conditions. The dissimilarity may stem from a lack of an appropriate reference state with the same charge and temperature for the BI-AdS black hole.

^{*}Electronic address: pengw@scu.edu.cn

[†]Electronic address: iverwu@scu.edu.cn

[‡]Electronic address: hyanga@scu.edu.cn

Contents

I. Introduction	2
II. NLED Black Hole in a Cavity	4
A. Black Hole Solution	4
B. Euclidean Action	7
C. Thermodynamics	8
III. Born-Infeld Black Hole in a Cavity	10
IV. Discussion and Conclusion	19
Acknowledgments	21
A. Reduced Action	21
References	23

I. INTRODUCTION

A Schwarzschild black hole in asymptotically flat space has negative specific heat and hence radiates more when it is smaller. To make this system thermally stable, appropriate boundary conditions must be imposed. One popular choice is putting the black hole in anti-de Sitter (AdS) space, which has a negative cosmological constant. The black hole becomes thermally stable since the AdS boundary acts as a reflecting wall. The thermodynamic properties of AdS black holes were first studied by Hawking and Page [1], who discovered the Hawking-Page phase transition, i.e., a phase transition between the thermal AdS space and the Schwarzschild-AdS black hole. Later, with the advent of the AdS/CFT correspondence [2–4], there has been much interest in studying the phase transitions of AdS black holes [5–10]. However, it is not clear whether the duality between the black hole and a boundary field theory is independent of the details of the boundary conditions, or just the special result of the asymptotically AdS space. It is therefore interesting to investigate thermodynamics of black holes in the case of different boundary conditions.

Alternatively, one can place the black hole inside a cavity in asymptotically flat space, on the wall of which the metric is fixed. In [11], York showed that a Schwarzschild black hole in a cavity can be thermally stable and experiences a Hawking-Page-like transition to the thermal flat space as the temperature decreases. Later, the thermodynamics of a Reissner-Nordstrom (RN) black hole in a cavity was discussed in a grand canonical ensemble [12] and a canonical ensemble [13, 14]. Similar to a RN-AdS black hole, it was found that a Hawking-Page-like phase transition occurs in the grand canonical ensemble, and a van der Waals-like phase transition occurs in the canonical ensemble. Note that a van der Waals-like phase transition consists of a first-order phase transition between two black hole phases of different sizes and a critical point, where the first-order phase transition ends, and a second order phase transition takes place. The phase structures of several black brane systems in a cavity were investigated in a series of paper [15–20], where Hawking-Page-like or van der Waals-like phase transitions were always found except for some special cases. Including charged scalars, boson stars and hairy black holes in a cavity were considered in [21–24], which showed that the phase structure of the gravity system in a cavity is strikingly similar to that of holographic superconductors in the AdS gravity. The stabilities of solitons, stars and black holes in a cavity were also studied in [25–32]. It was found that the nonlinear dynamical evolution of a charged black hole in a cavity could end in a quasi-local hairy black hole. Recently, McGough, Mezei and Verlinde [33] proposed that the $T\bar{T}$ deformed CFT_2 locates at the finite radial position of AdS_3 , which further motivates us to explore the properties of a black hole in a cavity.

Taking quantum contributions into account, nonlinear corrections are usually added to the Maxwell Lagrangian, which gives the nonlinear electrodynamics (NLED). Coupling NLED fields to gravity, various NLED charged black holes were derived and discussed in a number of papers [34–43]. It is interesting to note that some NLED black holes can be regular black hole models [44, 45]. As pointed out in [46], a globally regular NLED black hole requires vanishing electric charge and a finite NLED Lagrangian (or in the FP dual theory). Born-Infeld (BI) electrodynamics was first introduced to incorporate maximal electric fields and smooths divergences of the electrostatic self-energy of point charges [47]. Later, it is realized that BI electrodynamics can come from the low energy limit of string theory and encodes the low-energy dynamics of D-branes. The BI black hole solution was obtained in [48, 49]. The thermodynamic behavior and phase transitions of BI black holes in various gravities

were investigated in [50–62]. Especially, the thermodynamics of a 4D BI-AdS black hole was studied in [63–65], where a reentrant phase transition was always observed in a certain region of the parameter space.

In this paper, we first investigate the thermodynamic behavior of a 4D general NLED asymptotically flat black hole enclosed in a cavity. Then, we turn to study the phase structure and transition of a BI black hole in a cavity. We find that Hawking-Page-like and van der Waals-like phase transitions can occur while there is no reentrant phase transition. The rest of this paper is organized as follows. In section II, we compute the Euclidean action for the general NLED black hole in a cavity and discuss the thermodynamic properties of the system in the canonical ensemble. In section III, we focus on the BI black hole case to discuss the phase structure and transition. The phase diagrams of the BI black hole in a cavity is given in FIG. 1, from which one can read the black hole’s phase structure and transition. In the appendix, we present an alternative derivation of the Euclidean action for a general NLED black hole in a cavity using the reduced action method proposed in [12].

II. NLED BLACK HOLE IN A CAVITY

In this section, we consider a NLED charged black hole inside a cavity, on the boundary of which the temperature and charge are fixed. That said, the thermodynamics of the black hole is discussed in a canonical ensemble.

A. Black Hole Solution

First, we will consider the black hole solution in a $(3 + 1)$ dimensional model of gravity coupled to a nonlinear electromagnetic field A_μ . On a spacetime manifold \mathcal{M} with a time-like boundary $\partial\mathcal{M}$, the action is given by

$$\mathcal{S} = \int_{\mathcal{M}} d^4x \sqrt{-g} [R + \mathcal{L}(s, p)] + \mathcal{S}_{\text{surf}}, \quad (1)$$

where we take $16\pi G = 1$ for simplicity, $\mathcal{L}(s, p)$ is a general NLED Lagrangian, and $\mathcal{S}_{\text{surf}}$ are the surface terms on $\partial\mathcal{M}$. Here, s and p are two independent nontrivial scalars built from the field strength tensor $F_{\mu\nu} = \partial_\mu A_\nu - \partial_\nu A_\mu$ and none of its derivatives:

$$s = -\frac{1}{4}F^{\mu\nu}F_{\mu\nu} \text{ and } p = -\frac{1}{8}\epsilon^{\mu\nu\rho\sigma}F_{\mu\nu}F_{\rho\sigma}, \quad (2)$$

where $\epsilon^{\mu\nu\rho\sigma} \equiv -[\mu \ \nu \ \rho \ \sigma] / \sqrt{-g}$ is a totally antisymmetric Lorentz tensor, and $[\mu \ \nu \ \rho \ \sigma]$ is the permutation symbol. For later use, we define

$$G^{\mu\nu} = -\frac{\partial \mathcal{L}(s, p)}{\partial F_{\mu\nu}} = \mathcal{L}^{(1,0)}(s, p) F^{\mu\nu} + \frac{1}{2} \mathcal{L}^{(0,1)}(s, p) \epsilon^{\mu\nu\rho\sigma} F_{\rho\sigma}. \quad (3)$$

where we denote $\mathcal{L}^{(1,0)}(s, p) \equiv \frac{\partial \mathcal{L}(s, p)}{\partial s}$ and $\mathcal{L}^{(0,1)}(s, p) \equiv \frac{\partial \mathcal{L}(s, p)}{\partial p}$, respectively. Note that the general NLED theories with the Lagrangian $\mathcal{L}(s, p)$ were first considered in [66, 67]. The surface terms of the action (1) are

$$\mathcal{S}_{\text{surf}} = -2 \int_{\partial \mathcal{M}} d^3x \sqrt{-\gamma} (K - K_0) - \int_{\partial \mathcal{M}} d^3x \sqrt{-\gamma} n_\nu G^{\mu\nu} A_\mu. \quad (4)$$

The first term above is the Gibbons-Hawking-York surface term, where K is the extrinsic curvature, γ is the metric on the boundary, and K_0 is a subtraction term to make the Gibbons-Hawking-York term vanish in flat spacetime. When the metric on $\partial \mathcal{M}$ is fixed, the Gibbons-Hawking-York term is crucial to obtain the correct equations of motion from performing the variation. The second term, where n^μ is the unit outward-pointing normal vector of $\partial \mathcal{M}$, is included to keep the charge fixed on $\partial \mathcal{M}$, instead of the potential, when one varies the action to have the correct equations of motion [65]. Varying the action (1) in terms of $g_{\mu\nu}$ and A_μ with the metric and the charge fixed on $\partial \mathcal{M}$, we find that the equations of motion are

$$\begin{aligned} R_{\mu\nu} - \frac{1}{2} R g_{\mu\nu} &= \frac{T_{\mu\nu}}{2}, \\ \nabla_\mu G^{\mu\nu} &= 0, \end{aligned} \quad (5)$$

where $T_{\mu\nu}$ is the energy-momentum tensor for the NLED field:

$$T_{\mu\nu} = g_{\mu\nu} [\mathcal{L}(s, p) - p \mathcal{L}^{(0,1)}(s, p)] + \mathcal{L}^{(1,0)}(s, p) F_\mu{}^\rho F_{\nu\rho}. \quad (6)$$

We consider a static spherically symmetric black hole solution with the metric and the NLED field of the form

$$\begin{aligned} ds^2 &= -f(r) dt^2 + \frac{dr^2}{f(r)} + r^2 (d\theta^2 + \sin^2 \theta d\phi^2), \\ A &= A_t(r) dt. \end{aligned} \quad (7)$$

Moreover, we assume that the black hole lives in a spherical cavity, which has a boundary $\partial \mathcal{M}$ at $r = r_B$. The spacelike slices with constant t of $\partial \mathcal{M}$ are 2-spheres S^2 whose radii are

r_B . The equations of motion then reduce to

$$-1 + f(r) + r f'(r) = \frac{r^2}{2} [\mathcal{L}(s, 0) + A'_t(r) G^{rt}], \quad (8)$$

$$2f'(r) + r f''(r) = r \mathcal{L}(s, 0), \quad (9)$$

$$[r^2 G^{rt}]' = 0, \quad (10)$$

where

$$s = \frac{A_t'^2(r)}{2} \text{ and } G^{rt} = -\mathcal{L}^{(1,0)}(s, 0) A'_t(r). \quad (11)$$

It can show that eqn. (9) can be derived from eqns. (8) and (10).

Solving eqn. (10), we find that

$$G^{tr} = \frac{q}{r^2}, \quad (12)$$

where q is a constant. The charge of the system inside the cavity is defined as [65].

$$Q = -\frac{1}{4\pi} \int_{S^2} d^2x \sqrt{\sigma} n_\mu l_\nu G^{\mu\nu},$$

where l^μ is the unit normal vector of the constant t hypersurface, and σ is the induced metric on S^2 . Using eqn. (12), one finds that the charge inside the cavity becomes

$$Q = \frac{1}{4\pi} \int d\theta d\phi r_B^2 \sin\theta \frac{q}{r_B^2} = q. \quad (13)$$

From eqns. (11) and (12), $A'_t(r)$ is determined by

$$\mathcal{L}^{(1,0)}\left(\frac{A_t'^2(r)}{2}, 0\right) A'_t(r) = \frac{Q}{r^2}. \quad (14)$$

The gauge potential measured on $\partial\mathcal{M}$ with respect to the horizon is

$$\Phi = 4\pi \int_{r_+}^{r_B} A'_t(r) = \frac{4\pi A_t(r_B)}{\sqrt{f(r_B)}}, \quad (15)$$

where the blueshift factor $1/\sqrt{f(r_B)}$ relates A_t to the proper orthonormal frame component of the potential one-form A [12], and we fix the gauge field $A_t(r)$ at the horizon to be zero, i.e., $A_t(r_+) = 0$.

By integrating eqn. (8), we have

$$f(r) = 1 - \frac{M}{8\pi r} - \frac{1}{2r} \int_r^\infty dr r^2 \left[\mathcal{L}\left(\frac{A_t'^2(r)}{2}, 0\right) - A'_t(r) \frac{Q}{r^2} \right], \quad (16)$$

where M is the mass of the black hole [65]. Suppose that r_+ is the outer event horizon radius of the black hole. Since $f(r_+) = 0$, we can express $f(r)$ in terms of r_+ :

$$f(r) = 1 - \frac{r_+}{r} + \frac{1}{2r} \int_{r_+}^r dr r^2 \mathcal{L}\left(\frac{A_t'^2(r)}{2}, 0\right) - \frac{Q}{2r} A_t(r). \quad (17)$$

B. Euclidean Action

In the semiclassical approximation, one can relate the on-shell Euclidean action to the thermal partition function:

$$Z \simeq e^{-\mathcal{S}^E}, \quad (18)$$

where \mathcal{S}^E is the Euclidean continuation of the action \mathcal{S} : $\mathcal{S}^E = i\mathcal{S}$. The Euclidean time τ is obtained from Lorentzian time t by the analytic continuation $t = i\tau$. From $A_\tau d\tau = A_t dt$, it follows that

$$A_\tau = -iA_t, \quad (19)$$

which gives $G_{r\tau} = -iG_{rt}$. So eqn. (12) becomes

$$G_{r\tau} = -i\frac{Q}{r^2}. \quad (20)$$

Moreover, the gauge potential on $\partial\mathcal{M}$ is

$$\Phi = \frac{4\pi i A_\tau(r_B)}{\sqrt{f(r_B)}}. \quad (21)$$

Since the temperature T is fixed on the boundary of the cavity, we can impose the boundary condition at $r = r_B$ in terms of the reciprocal temperature:

$$\int \sqrt{f(r_B)} d\tau = T^{-1}. \quad (22)$$

which identifies the Euclidean time τ as $\tau \sim \tau + \frac{1}{T\sqrt{f(r_B)}}$, and hence the period of τ is $\frac{1}{T\sqrt{f(r_B)}}$.

For the black hole solution (7), one can evaluate the Euclidean action by integrating over angles and performing the integration by parts:

$$\begin{aligned} \mathcal{S}^E = & -\frac{8\pi}{T\sqrt{f(r_B)}} \int_{r_+}^{r_B} dr [f(r) + 1 + rf'(r)] + \frac{16\pi r_B}{T} \\ & - 16\pi^2 r_+^2 - \frac{4\pi}{T\sqrt{f(r_B)}} \int_{r_+}^{r_B} dr r^2 \mathcal{L} \left(-\frac{A_\tau^2(r)}{2}, 0 \right) + \frac{4\pi i A_\tau(r_B) Q}{T\sqrt{f(r_B)}}. \end{aligned} \quad (23)$$

After eqn. (17) is plugged into eqn. (23), a straightforward calculation gives

$$\mathcal{S}^E = \frac{16\pi r_B}{T} [1 - \sqrt{f(r_B)}] - S, \quad (24)$$

where $S = 16\pi^2 r_+^2$ is the entropy of the black hole.

For large values of r_B , one finds that

$$f(r_B) = 1 - \frac{M}{8\pi r_B} + \frac{Q^2}{4r_B^2} + \mathcal{O}(r_B^{-4}). \quad (25)$$

In the limit of $r_B \rightarrow \infty$, the Euclidean action then reduces to

$$\mathcal{S}^E = \frac{1}{T} (M - TS), \quad (26)$$

as expected.

C. Thermodynamics

Various thermodynamic quantities can be derived from the Euclidean action (24), which is related to the free energy F in the semiclassical approximation by

$$F = -T \ln Z = T\mathcal{S}^E. \quad (27)$$

From eqns. (17) and (24), one finds that the free energy F is a function of the temperature T , the charge Q , the cavity radius r_B and the horizon radius r_+ :

$$F = F(r_+; T, Q, r_B), \quad (28)$$

where T , Q and r_B are parameters of the canonical ensemble. The only variable r_+ can be determined by extremizing the free energy $F(r_+; T, Q, r_B)$ with respect to r_+ :

$$\frac{dF(r_+; T, Q, r_B)}{dr_+} = 0 \implies -\frac{d[r_B f(r_B)]/dr_+}{2\sqrt{f(r_B)}} = 2\pi r_+ T \implies f'(r_+) = 4\pi T \sqrt{f(r_B)}, \quad (29)$$

where we use $d[r_B f(r_B)]/dr_+ = -r_+ f'(r_+)$. That said, the solution $r_+ = r_+(T, Q, r_B)$ of eqn. (29) corresponds to a locally stationary point of $F(r_+; T, Q, r_B)$. It is interesting to note that eqn. (29) can be written as

$$T = \frac{T_h}{\sqrt{f(r_B)}}, \quad (30)$$

where

$$T_h = \frac{f'(r_+)}{4\pi} = \frac{1}{4\pi r_+} \left\{ 1 + \frac{r_+^2}{2} \mathcal{L} \left(\frac{A_t'^2(r_+)}{2}, 0 \right) - \frac{A_t'(r_+) Q}{2} \right\}, \quad (31)$$

is the Hawking temperature of the black hole. The temperature T on $\partial\mathcal{M}$ is thus blueshifted from T_h , which is measured at infinity.

After obtained $r_+ = r_+(T, Q, r_B)$, we can evaluate $F(r_+; T, Q, r_B)$ at the locally stationary point $r_+ = r_+(T, Q, r_B)$:

$$F(T, Q, r_B) \equiv F(r_+(T, Q, r_B); T, Q, r_B). \quad (32)$$

For later convenience, we shall suppress T, Q and r_B in $F(r_+; T, Q, r_B)$ and $F(T, Q, r_B)$ and denote $F(r_+; T, Q, r_B)$ and $F(T, Q, r_B)$ as $F(r_+)$ and F , respectively. The thermal energy of the black hole in the cavity is

$$E = -T^2 \frac{\partial(F/T)}{\partial T} = 16\pi r_B \left[1 - \sqrt{f(r_B)} \right]. \quad (33)$$

Using eqn. (16), we can express the ADM mass of the black hole M in terms of E and Q :

$$M = E - \frac{E^2}{32\pi r_B} - 4\pi \int_{r_B}^{\infty} dr r^2 \left[\mathcal{L} \left(\frac{A_t^2(r)}{2}, 0 \right) - A_t'(r) \frac{Q}{r^2} \right], \quad (34)$$

where the second and third terms on left-hand side can be interpreted as the gravitational and electrostatic binding energies, respectively. Using eqn. (17), we can express the thermal energy E in terms of the entropy S , the charge Q and the cavity radius r_B . Differentiating E with respect to S and Q , respectively, gives

$$\begin{aligned} \frac{\partial E}{\partial S} &= -\frac{d[r_B f(r_B)]/dr_+}{4\pi r_+ \sqrt{f(r_B)}} = T, \\ \frac{\partial E}{\partial Q} &= -\frac{8\pi r_B}{\sqrt{f(r_B)}} \frac{\partial f(r_B)}{\partial Q} = \Phi. \end{aligned} \quad (35)$$

From the energy E , we can define a thermodynamic surface pressure by

$$\lambda \equiv -\frac{\partial E}{\partial(4\pi r_B^2)} = \frac{\left(1 - \sqrt{f(r_B)}\right)^2}{r_B \sqrt{f(r_B)}} + \frac{r_B^2 \mathcal{L} \left(\frac{A_t^2(r_B)}{2}, 0 \right) - Q A_t'(r_B)}{2r_B \sqrt{f(r_B)}}. \quad (36)$$

From eqns. (35) and (36), the first law of thermodynamics can be established:

$$dE = TdS + \Phi dQ - \lambda dA, \quad (37)$$

where $A \equiv 4\pi r_B^2$ is the surface area of the cavity.

To obtain the proper Smarr relation for the black hole, we need to consider the dimensional couplings a_i in the NLED Lagrangian $\mathcal{L}(s, p)$, which have $[a_i] = L^{c_i}$. Since the dimensional analysis give that $[Q] = [M] = L$, $[T] = [\lambda] = L^{-1}$ and $[A] = [S] = L^2$, the Euler scaling argument leads to the Smarr relation

$$M = 2(TS - \lambda A) + \sum_i c_i a_i \mathcal{A}_i + Q\Phi, \quad (38)$$

where we introduce the conjugates \mathcal{A}_i associated with a_i :

$$\mathcal{A}_i = \frac{\partial M}{\partial a_i}. \quad (39)$$

We now discuss the thermodynamic stability of the black hole in the cavity against thermal fluctuations. In the canonical ensemble, one considers the specific heat at constant electric charge:

$$C_Q = T \left(\frac{\partial S}{\partial T} \right)_Q = 32\pi^2 r_+(T, Q, r_B) T \frac{\partial r_+(T, Q, r_B)}{\partial T}. \quad (40)$$

When $C_Q > 0$, the system is thermally stable. Thus, a thermally stable black hole phase has $\frac{\partial r_+(T, Q, r_B)}{\partial T} > 0$. Since $\partial^2 F / \partial^2 T = -C_Q$, the thermally stable/unstable phases have concave downward/upward F - T curves. On the other hand, it can show that, at $r_+ = r_+(T, Q, r_B)$,

$$\frac{\partial^2 F(r_+)}{\partial r_+^2} = \frac{32\pi^2 r_+}{\partial r_+ / \partial T}, \quad (41)$$

which means that the black hole phase is thermally stable/unstable if $r_+(T, Q, r_B)$ is a local minimum/maximum of $F(r_+)$.

To find the global minimum of $F(r_+)$ over the space of the variable r_+ with fixed values of T, Q and r_B , we also need to consider the values of $F(r_+)$ at the edges of the space of r_+ . In fact, the physical space of r_+ is constrained by

$$r_e \leq r_+ \leq r_B, \quad (42)$$

where r_e is the horizon radius of the extremal black hole with the charge being Q . If there exists no extremal black hole solution for Q , one can simply set $r_e = 0$. For simplicity, the global minimum of $F(r_+)$ at the edges is dubbed "edge state (ES)" in our paper.

III. BORN-INFELD BLACK HOLE IN A CAVITY

BI electrodynamics is described by the Lagrangian density

$$\mathcal{L}(s, p) = \frac{1}{a} (1 - \sqrt{1 - 2as}), \quad (43)$$

where the coupling parameter a is related to the string tension α' as $a = (2\pi\alpha')^2 > 0$. For $a = 0$, the BI Lagrangian would reduce to the Maxwell Lagrangian. Solving eqn. (14) for $A'_t(r)$ gives

$$A'_t(r) = \frac{Q}{\sqrt{r^4 + aQ^2}}, \quad (44)$$

where Q is the charge of the BI black hole. From eqn. (17), one can express $f(r)$ in terms of the horizon radius r_+ :

$$f(r) = 1 - \frac{r_+}{r} + \frac{r_+}{r} \frac{Q^2}{6\sqrt{r_+^4 + aQ^2} + 6r_+^2} - \frac{Q^2}{3rr_+} {}_2F_1\left(\frac{1}{4}, \frac{1}{2}, \frac{5}{4}; -\frac{aQ^2}{r_+^4}\right) - \frac{Q^2}{6\sqrt{r^4 + aQ^2} + 6r^2} + \frac{Q^2}{3r^2} {}_2F_1\left(\frac{1}{4}, \frac{1}{2}, \frac{5}{4}; -\frac{aQ^2}{r^4}\right), \quad (45)$$

where ${}_2F_1(a, b, c; x)$ is the hypergeometric function.

It is convenient to express quantities in units of r_B :

$$x \equiv \frac{r_+}{r_B}, \quad \tilde{Q} \equiv \frac{Q}{r_B}, \quad \tilde{a} \equiv \frac{a}{r_B^2}, \quad \tilde{T} \equiv r_B T, \quad \tilde{F}(x) = \frac{F(r_+)}{16\pi r_B} \text{ and } \tilde{F} = \frac{F}{16\pi r_B}, \quad (46)$$

where r_+ is the horizon radius. We then use eqns. (24) and (45) to find the free energy as a function of x :

$$\tilde{F}(x) = 1 - \sqrt{f(x)} - \pi x^2 \tilde{T}, \quad (47)$$

where

$$f(x) = 1 - x + \frac{x\tilde{Q}^2}{6\sqrt{x^4 + \tilde{a}\tilde{Q}^2} + 6x^2} - \frac{\tilde{Q}^2}{3x} {}_2F_1\left(\frac{1}{4}, \frac{1}{2}, \frac{5}{4}; -\frac{\tilde{a}\tilde{Q}^2}{x^4}\right) - \frac{\tilde{Q}^2}{6\sqrt{1 + \tilde{a}\tilde{Q}^2} + 6} + \frac{\tilde{Q}^2}{3} {}_2F_1\left(\frac{1}{4}, \frac{1}{2}, \frac{5}{4}; -\tilde{a}\tilde{Q}^2\right). \quad (48)$$

The Hawking temperature of the BI black hole can be calculated from eqn. (31):

$$\tilde{T}_h \equiv r_B T_h = \frac{1}{4\pi x} \left(1 - \frac{1}{2} \frac{\tilde{Q}^2}{x^2 + \sqrt{x^4 + \tilde{a}\tilde{Q}^2}} \right). \quad (49)$$

The locally stationary points of $\tilde{F}(x)$ are determined by $d\tilde{F}(x)/dx = 0$, which becomes

$$\tilde{T} = \frac{\tilde{T}_h}{\sqrt{f(x)}}. \quad (50)$$

As shown in [37], there are two types of BI black holes depending on the minimum value of \tilde{T}_h :

- RN type: $4\tilde{a} \leq \tilde{Q}^2 \leq 4(1 + \tilde{a})$. This type of BI black holes can have extremal black hole solutions like RN black holes. In fact, the Hawking temperature $\tilde{T}_h = 0$ has one single solution $x = x_e \equiv \frac{1}{2}\sqrt{\tilde{Q}^2 - 4\tilde{a}}$, where $x_e r_B$ is the horizon radius of the extremal

BI black hole with Q and a . In this case, we must have $x_e \leq x \leq 1$. Note that requiring $x_e \leq 1$ puts an upper bound on \tilde{Q}^2 : $\tilde{Q}^2 \leq 4(1 + \tilde{a})$. Another way to understand this upper bound is that, when $\tilde{Q}^2 > 4(1 + \tilde{a})$, $f(x)$ is always negative and hence $\tilde{F}(x)$ is not a real-valued function for any x . When $x = x_e$ we have an extremal BI black hole, and when $x = 1$ the horizon merges with the boundary.

- Schwarzschild-like type: $\tilde{Q}^2 < 4\tilde{a}$. This type of BI black holes have only one horizon like Schwarzschild black holes. The Hawking temperature \tilde{T}_h has a positive minimum value and goes to $+\infty$ as $x \rightarrow 0$. In this case, we can have $0 \leq x \leq 1$, over which $\tilde{F}(x)$ is well-defined. It can show that $\tilde{T}_h/\sqrt{f(x)}$ has a minimum value of $\tilde{T}_{\min} > 0$ over $0 \leq x \leq 1$. Eqn. (50) implies that the locally stationary points of $\tilde{F}(x)$, corresponding to BI black hole solutions, only exist for $\tilde{T} \geq \tilde{T}_{\min}$. When $x = 0$, one finds that eqn. (45) becomes

$$f(r) = 1 - \frac{Q^{3/2}\Gamma(1/4)\Gamma(5/4)}{3a^{1/4}\sqrt{\pi}r} - \frac{Q^2}{6\sqrt{r^4 + aQ^2} + 6r^2} + \frac{Q^2}{3r^2} {}_2F_1\left(\frac{1}{4}, \frac{1}{2}, \frac{5}{4}; -\frac{aQ^2}{r^4}\right). \quad (51)$$

If $Q = 0$, $f(r) = 1$, and hence the edge state at $x = 0$ is just the thermal flat space. For $Q > 0$, we have

$$f(r) = 1 - \frac{Q}{2\sqrt{a}} + \mathcal{O}(r) \quad \text{and} \quad R = \frac{Q}{\sqrt{a}r^2} - \frac{2}{a} + \mathcal{O}(r), \quad (52)$$

where R is the Ricci scalar. So the metric has a physical singularity at $r = 0$ although $f(0)$ is finite. It can show that $f(r) > 0$, and hence there exists no horizon. The edge state with $Q > 0$ at $x = 0$ is thus a naked singularity.

To find the phase structure and transition of a BI black hole in a cavity, we need to analyze the locally stationary points of $\tilde{F}(x)$ and find the global minimum value of $\tilde{F}(x)$. In fact, with fixed value of \tilde{a} , the locally stationary points of $\tilde{F}(x)$ can be determined by solving eqns. (30) and (49) for x in terms of \tilde{T} and \tilde{Q} . The solution $x(\tilde{T}, \tilde{Q})$ is often a multivalued function, each branch of which corresponds to a family of BI black hole solutions. When $x(\tilde{T}, \tilde{Q})$ is multivalued, there is more than one family of BI black holes of different sizes with fixed values of \tilde{T} and \tilde{Q} . We find that there are five regions in the \tilde{a} - \tilde{Q} phase space of the BI black hole, in each of which the BI black hole has distinct behavior of the branches of $x(\tilde{T}, \tilde{Q})$ and phase structure. The five regions of the \tilde{a} - \tilde{Q} phase space are mapped in FIG.

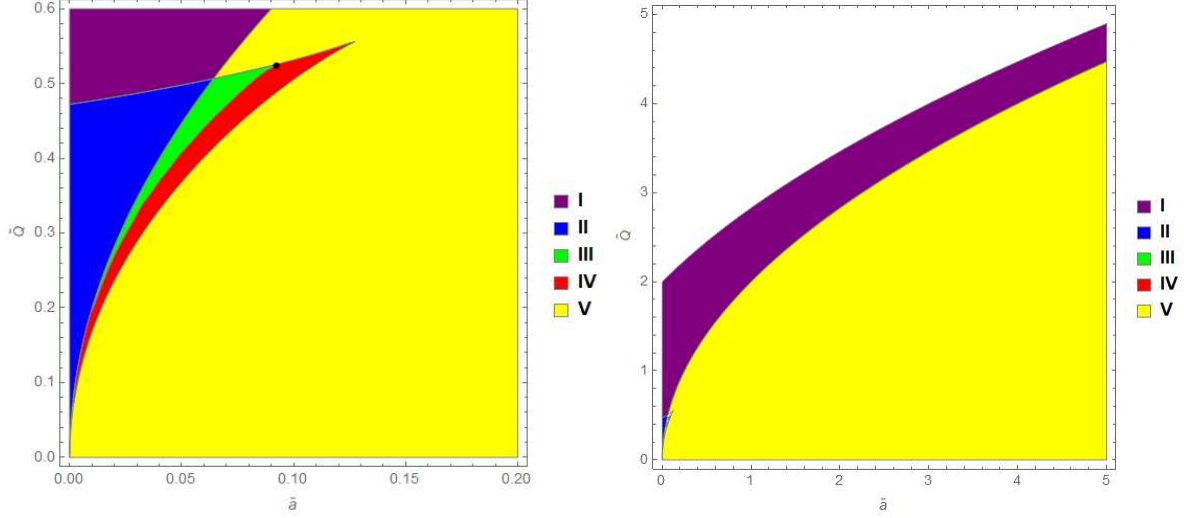


FIG. 1: The five regions in the \tilde{a} - \tilde{Q} phase space of a BI black hole (BH) in a cavity, each of which possesses distinct behavior of the phase structure and transition. Varying the temperature, a van der Waals-like LBH/SBH phase transition occurs in Regions II and III while a Hawking-Page-like ES/BH phase transition occurs in Regions III, IV and V. There is only one phase in Regions I. The critical line consists of $\tilde{Q}_{12}(\tilde{a})$ and $\tilde{Q}_{35}(\tilde{a})$, where $\tilde{Q}_{ij}(\tilde{a})$ is the boundary Region i and Region j . The critical line terminates at the black dot, which is at $\{\tilde{a}_c, \tilde{Q}_c\} \approx \{0.092, 0.524\}$.

1. We plot $x(\tilde{T}, \tilde{Q})$ against \tilde{T} for various values of \tilde{Q} with $\tilde{a} = 0.05$ in FIG. 2, which shows the general behavior of $x(\tilde{T}, \tilde{Q})$ in these five regions. In what follows, we discuss the phase structure and transition of the BI black hole in the five regions:

- Region I: As shown in FIG. 2, there is only one branch for $x(\tilde{T}, \tilde{Q})$ with fixed values of \tilde{a} and \tilde{Q} , on which the BI black hole is thermally stable. Since BI black holes in this region satisfy $\tilde{Q} \geq 4\tilde{a}$, they are RN type, and hence \tilde{T} can go to zero. For the BI black hole with $\tilde{a} = 0.01$ and $\tilde{Q} = 0.6$ in this region, we plot the free energy $\tilde{F}(x)$ in FIG. 3(a), which shows that the endpoints always have higher free energy, and the local minimum of $\tilde{F}(x)$ is also the global minimum. There is only one phase in this region.
- Region II: BI black holes in this region are RN type. As shown in FIG. 2, there are three branches for $x(\tilde{T}, \tilde{Q})$ with fixed values of \tilde{a} and \tilde{Q} , which are denoted by Small BH (green), Large BH (blue) and Intermediate BH (brown). Both the Small BH and

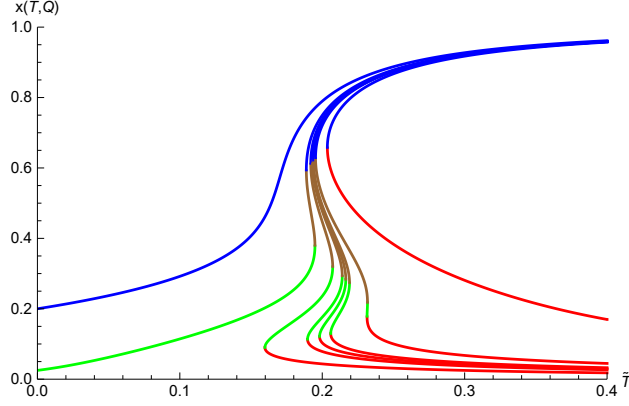
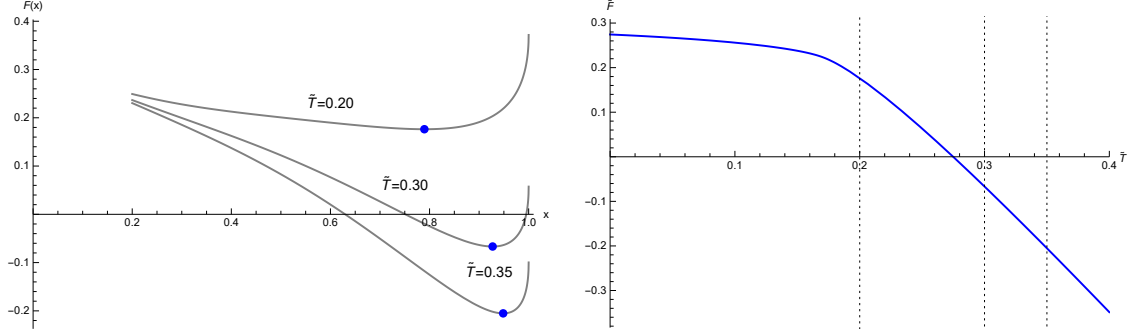


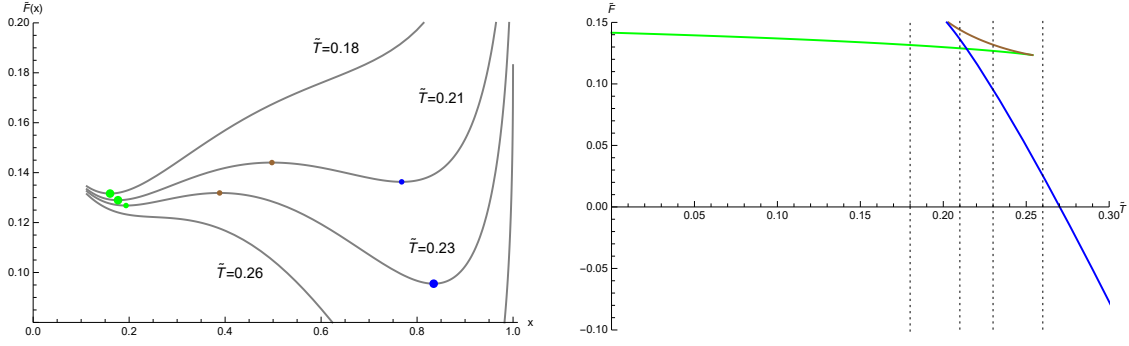
FIG. 2: Plots of $x(\tilde{T}, \tilde{Q})$ against \tilde{T} for various values of \tilde{Q} with $\tilde{a} = 0.05$, where $x(\tilde{T}, \tilde{Q})$ is the locally stationary point of $\tilde{F}(x)$. From left to right, $\tilde{Q} = 0.600$ (Region I), 0.450 (Region II), 0.415 (Region III), 0.400 (Region IV), 0.395 (Region IV), 0.390 (Region IV), 0.370 (Region IV) and 0.200 (Region V). Since thermally stable phases have $\partial x / \partial \tilde{T} > 0$, the BI BHs on blue and green segments of the curves are thermally stable. We denote the BI BHs on blue segments by Large BH (or BH if there is no green segment on the curve) and these on green segments by Small BH. The BI BHs on red and brown segments are denoted by Intermediate BH, which are thermally unstable.

Large BH branches are thermally stable. For the BI black hole with $\tilde{a} = 0.01$ and $\tilde{Q} = 0.3$ in this region, we plot the free energy $\tilde{F}(x)$ in FIG. 3(b), which shows that the endpoints always have higher free energy than the global minimum. $\tilde{F}(x)$ has the global minimum at Small BH for small enough \tilde{T} and Large BH for large enough \tilde{T} , respectively. The free energies of the three branches are plotted in the right panel of FIG. 3(b), which shows that there is a first-order phase transition between Small BH and Large BH.

- Region III: BI black holes in this region are Schwarzschild-like type. For $\tilde{T} < \tilde{T}_{\min}$, $\tilde{F}(x)$ is a strictly increasing function (see $\tilde{T} = 0.10$ in the left panel of FIG. 4), and hence $\tilde{F}(x)$ has the global minimum at $x = 0$, dubbed the edge state. For $\tilde{T} \geq \tilde{T}_{\min}$, as shown in FIG. 2, there are four branches for $x(\tilde{T}, \tilde{Q})$ with fixed values of \tilde{a} and \tilde{Q} , which are denoted by Small BH (green), Large BH (blue) and Intermediate BH (brown and red). Both the Small BH and Large BH branches are thermally stable. The free energies of the four branches and the edge state are plotted in the right panel of FIG. 4. As \tilde{T} increases from \tilde{T}_{\min} , the free energy of Small BH decrease while $\tilde{F}(0)$



(a) Region I: $\tilde{a} = 0.01$ and $\tilde{Q} = 0.6$. There is no phase transition.



(b) Region II: $\tilde{a} = 0.01$ and $\tilde{Q} = 0.3$. There is a first-order phase transition between Small BH and Large BH.

FIG. 3: Plots of the free energies $\tilde{F}(x)$ and \tilde{F} against \tilde{T} for the BI BHs in Regions I and II. The BI BHs in these regions are RN type. The BI BHs on the blue and green branches (dots) are thermally stable. **Left Panels:** $\tilde{F}(x)$ is plotted for various values of \tilde{T} , which are depicted by the vertical black dotted lines in the right panels. The locally stationary points of $\tilde{F}(x)$ are marked with colored dots, the colors of which correspond to these of segments in FIG. 2. Larger dots represent global minimums of $\tilde{F}(x)$, which are globally stable. **Right Panels:** The values of $\tilde{F}(x)$ evaluated at the locally stationary points are plotted against \tilde{T} . Their colors match these in the left panels and FIG. 2, which means that blue/green branches are Large/Small BH, and the brown branch is Intermediate BH.

is constant. They cross each other at some point, where a first-order transition occurs, and Small BH becomes globally stable. Further increasing \tilde{T} , Large BH appears, and its free energy decrease more rapidly than that of Small BH. So they cross each other at some point, where another first-order transition occurs, and Large BH then becomes the globally stable one.

- Region IV: BI black holes in this region are also Schwarzschild-like type. As in Region III, the edge state at $x = 0$ is globally stable for $\tilde{T} < \tilde{T}_{\min}$. For $\tilde{T} \geq \tilde{T}_{\min}$, there are also

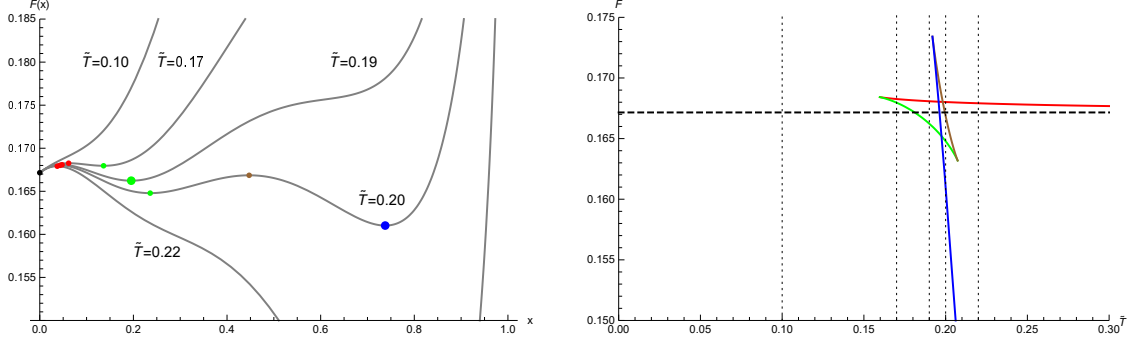
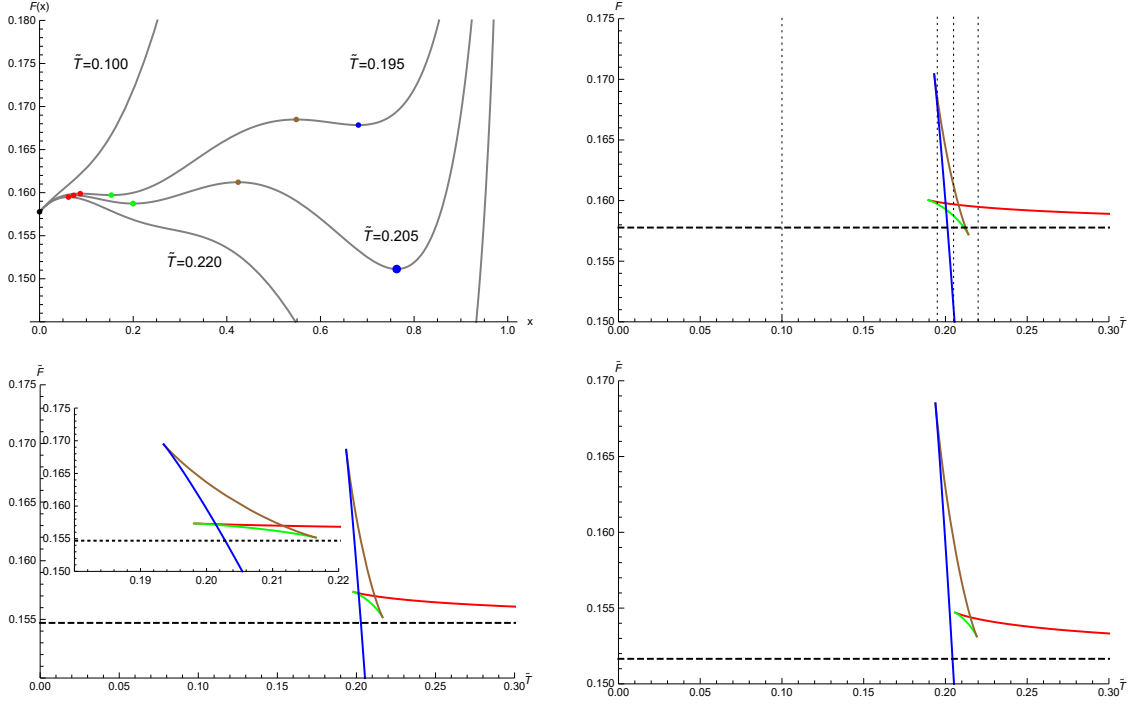


FIG. 4: Region III: $\tilde{a} = 0.05$ and $\tilde{Q} = 0.415$. The BI BHs in this region are Schwarzschild-like type, which implies that x can go to 0. **Left Panel:** The locally stationary points of $\tilde{F}(x)$ are represented with colored dots, and $\tilde{F}(0)$ is marked with the black dot. Larger colored dots represent global minimums of $\tilde{F}(x)$. If there is no larger colored dot for some \tilde{T} , $\tilde{F}(x)$ has the global minimum at $x = 0$. **Right Panel:** The colored branches are the values of $\tilde{F}(x)$ evaluated at the locally stationary points as functions of \tilde{T} . Specifically, the blue/green branches are Large/Small BH, and the brown/red branches are Intermediate BH. The horizontal black dashed line is $\tilde{F}(0)$. As \tilde{T} increases from zero, a first-order phase transition from the edge state to Small BH occurs at some \tilde{T} . Further increasing \tilde{T} , there would be another first-order phase transition from Small BH to Large BH.

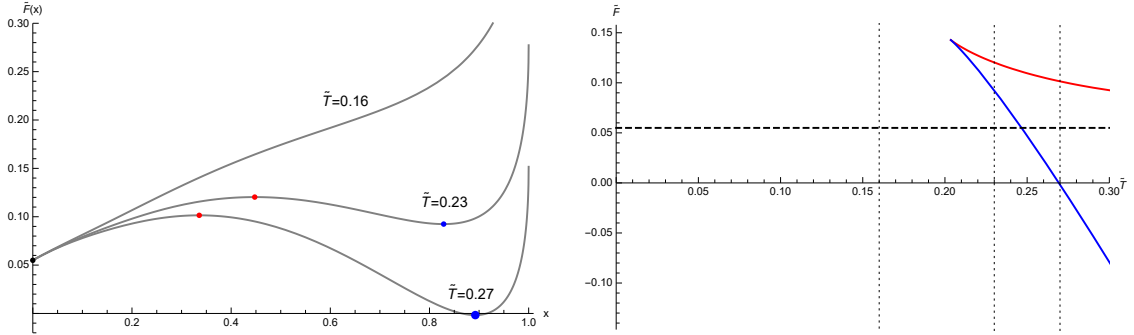
four branches for $x(\tilde{T}, \tilde{Q})$ with fixed values of \tilde{a} and \tilde{Q} , which are denoted by Small BH (green), Large BH (blue) and Intermediate BH (brown and red). The free energies of the four branches and the edge state are plotted in FIG. 5(a). Unlike Region III, the temperature at which Small BH appears is too high, such that $\tilde{F}(0)$ does not cross the free energy of Small BH or $\tilde{F}(0)$ crosses the free energy of Large BH before it crosses that of Small BH. Hence as \tilde{T} increases, there is only one first-order transition from the edge state to Large BH at some temperature, where the free energy of Large BH and $\tilde{F}(0)$ cross each other.

- Region V: BI black holes in this region are also Schwarzschild-like type. As in Regions III and IV, the edge state at $x = 0$ is globally stable for $\tilde{T} < \tilde{T}_{\min}$. However for $\tilde{T} \geq \tilde{T}_{\min}$, there are two branches for $x(\tilde{T}, \tilde{Q})$ with fixed values of \tilde{a} and \tilde{Q} , which are denoted by BH (green) and Intermediate BH (red). The BH branch is thermally stable. The free energies of the two branches and the edge state are plotted in FIG. 5(b), which shows that there is a first-order transition from the edge state to Large



(a) Region IV: $\tilde{a} = 0.05$. Top Panels: $\tilde{Q} = 0.400$. Bottom-Left Panel: $\tilde{Q} = 0.395$. Bottom-Right Panel:

$\tilde{Q} = 0.390$.



(b) Region V: $\tilde{a} = 0.05$ and $\tilde{Q} = 0.4$.

FIG. 5: Plots of the free energies $\tilde{F}(x)$ and \tilde{F} against \tilde{T} for the BI BHs in Regions IV and V, which are Schwarzschild-like type. The blue/green branches are Large/Small BH, and the brown/red branches are Intermediate BH. The horizontal black dashed line is $\tilde{F}(0)$. As \tilde{T} increases from zero, there is always a single first-order phase transition from the edge state to Large BH occurring at some temperature.

BH as \tilde{T} increases.

In FIG. 1, the boundary between the region in which $x(\tilde{T}, \tilde{Q})$ has n branches and that in which $x(\tilde{T}, \tilde{Q})$ has $n + 2$ branches is the critical line. There are 3 such boundaries in

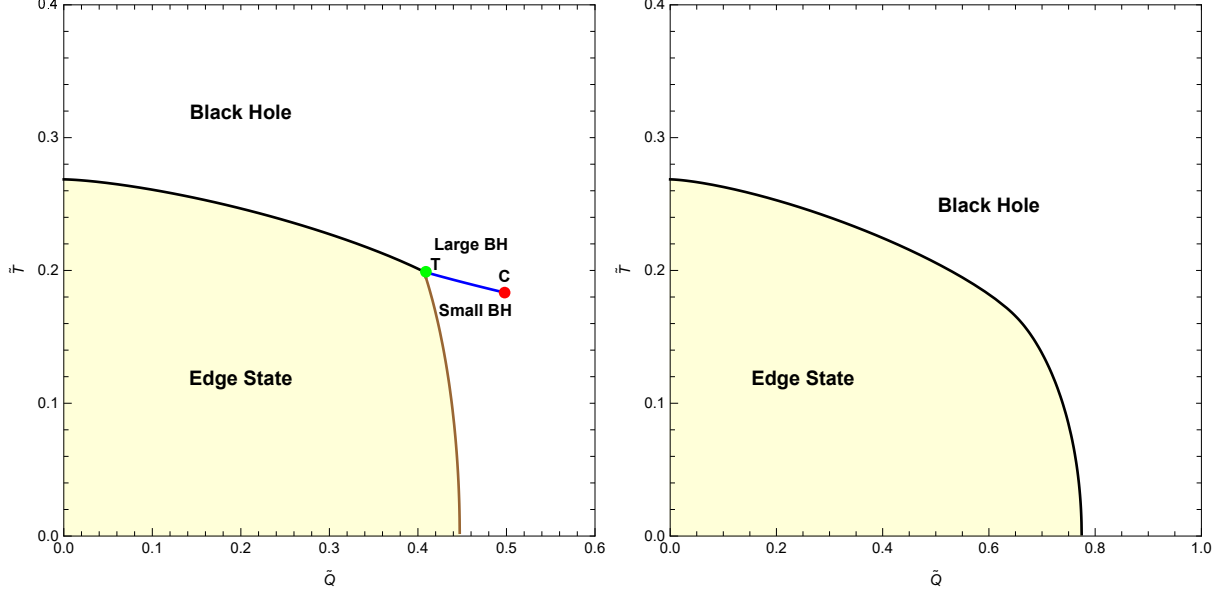


FIG. 6: The phase diagrams in the \tilde{Q} - \tilde{T} phase space. **Left Panel:** $\tilde{a} = 0.05 < \tilde{a}_c$. The first-order phase transition line separating Large BH and Small BH is displayed by the blue line, and it terminates at the critical point, marked by the red dot and annotated by C. There are also a first-order phase transition line between BH and the edge state, depicted by the black line, and a first-order phase transition line between SBH and the edge state, depicted by the brown line. These first-order phase transition lines merge together at the tricritical point, marked by the green dot and annotated by T. **Right Panel:** $\tilde{a} = 0.15 > \tilde{a}_c$. There is a first-order phase transition line separating BH and the edge state, displayed by the black line.

FIG. 1, i.e., $\tilde{Q}_{12}(\tilde{a})$, $\tilde{Q}_{35}(\tilde{a})$ and $\tilde{Q}_{45}(\tilde{a})$, where $\tilde{Q}_{ij}(\tilde{a})$ is the boundary between Region i and Region j . However, FIG. 5 shows that $\tilde{Q}_{45}(\tilde{a})$ is not physical since it does not globally minimize the free energy. Thus physical critical line only consists of $\tilde{Q}_{12}(\tilde{a})$ and $\tilde{Q}_{35}(\tilde{a})$, which terminates at $\{\tilde{a}_c, \tilde{Q}_c\} \simeq \{0.092, 0.524\}$. The line $\tilde{Q}_{12}(\tilde{a})$ is reminiscent of RN black holes.

The phase diagram with $\tilde{a} = 0.05$ in the \tilde{Q} - \tilde{T} phase space is displayed in the left panel of FIG. 6. There is a LBH/SBH first-order phase transition for some range of \tilde{Q} , a Hawking-Page-like ES/SBH first-order phase transition for some smaller range of \tilde{Q} and another Hawking-Page-like ES/BH first-order phase transition for some larger range of \tilde{Q} . The LBH/SBH phase transition line is a van der Waals-like phase transition and hence terminates at the critical point, represented by the red dot. These three first-order phase transition lines merge together at the tricritical point, marked by the green dot. The phase diagram

with $\tilde{a} = 0.15$ in the \tilde{Q} - \tilde{T} phase space is plotted in the right panel of FIG. 6, which is simpler than that with $\tilde{a} = 0.05$. Since $\tilde{a} = 0.15 > \tilde{a}_c$, there is no critical point or tricritical point in this phase diagram. There are two phases, namely the edge state and BH, which are separated by a Hawking-Page-like first-order phase transition line.

IV. DISCUSSION AND CONCLUSION

In the first part of this paper, we calculated the Euclidean action of a general NLED black hole in a finite spherical cavity and investigated the corresponding thermodynamic behavior in a canonical ensemble. Specifically, the Euclidean action was given by eqn. (24), which could be interpreted as the free energy of the black hole. It was then demonstrated that the first law of thermodynamics and the Smarr relation were satisfied at the locally stationary points of the free energy. It also showed that the local minimum of the free energy corresponds to the locally stable phase of the system. To determine the globally stable phase, the edge states are needed to be considered as well.

In the second part, we examined the phase structure and transition of a BI black hole in a cavity. In FIG. 1, we mapped five regions in the \tilde{a} - \tilde{Q} phase space, each of which has different phase behavior. Regions I and II are reminiscent of RN black holes, where there exist extremal black hole solutions. In these two regions, the global minimum of the free energy is always at one of the locally stationary points. There is only one branch of black hole solutions in Region I, while in Region II, there is a band of temperatures where three branches coexist, and a first-order LBH/SBH phase transition occurs. In Regions III, IV and V, for low temperatures, the global minimum of the free energy is at $x = 0$, which describes a naked singularity. For high enough temperatures, the global minimum is at one of the locally stationary points, and hence there is a first-order phase transition from the edge state at $x = 0$ to the black hole phase as the temperature increases. In Region III, further increasing the temperature will lead to another first-order phase transition from Small BH to Large BH. The phase diagrams with $\tilde{a} = 0.05$ and 0.15 in the \tilde{Q} - \tilde{T} phase space were plotted in FIG. 6, respectively. For $\tilde{a} = 0.05$, there are three first-order phase transition lines merging together at a tricritical point. At the critical temperature, there is a critical point, corresponding to a second-order phase transition, beyond which there is only one phase. For $\tilde{a} = 0.15$, there is only one phase transition line, which separates the edge state

from the black hole phase. Note that we only focus on spherical topology in our paper, so it is possible that there are some other states of lower free energy in a different topological sector with the same charge and temperature. If this happens, the stable phases discussed above are only metastable.

Using asymptotically AdS boundary conditions, the thermodynamics of BI black holes was considered in [63–65]. For the RN type in Regions I and II, the phase structure of a BI black hole in a cavity is analogous to that of the corresponding BI-AdS black hole. However for the Schwarzschild-like type in Regions III, IV and V, we find that there are some differences between the thermodynamics of the BI black holes under these two boundary conditions. For example, a LBH/SBH/LBH reentrant phase transition, which consists of a LBH/SBH first-order phase transition and a LBH/SBH zeroth-order phase transition, could occur for the BI-AdS black holes in Region V of [65]. On the other hand, such reentrant phase transition is not observed for any BI black hole in a cavity. Nevertheless, it is naive to claim that the phase structure of BI black holes depends on details of the boundary conditions. A crucial observation is that, if there were no edge states, the phase structure of the BI black hole in a cavity would be quite similar to that of the BI-AdS black hole. In fact, if the edge state is ignored, the inset of the bottom left panel in FIG. 5(a) shows that, as the temperature increases, there is a finite jump in free energy leading to a zeroth-order phase transition from Large BH to Small BH, which is followed by a first-order phase transition returning to Large BH. This LBH/SBH/LBH transition is just the reentrant phase transition.

In asymptotically AdS spaces, the Euclidean action needs to be regulated to cancel the divergences coming from the asymptotic region. One can use the background-subtraction method to regularize the Euclidean action by subtracting a contribution from a reference background. The reference background and the edge state play a similar role in determining the global minimum of the free energy. For a Schwarzschild-AdS black hole, the reference background is just the thermal flat space, which is the same as the edge state at $x = 0$ for a Schwarzschild black hole in a cavity. As the temperature decreases, both the Schwarzschild black hole in a cavity and the Schwarzschild-AdS black hole thus experience the Hawking-Page transition to the thermal flat space [11]. Although there is ambiguity about the reference background of charged black holes, one can circumvent this by using the counterterm subtraction method [68, 69], in which the Euclidean action is regularized in a

background-independent fashion by adding a series of boundary counterterms to the action. In [63, 65], the counterterm subtraction method was used to compute the Euclidean action for a BI-AdS black hole. For a RN black hole in a cavity, the global minimum of the free energy is never at the endpoints, which explains that the phase structures of the RN black hole in a cavity and the RN-AdS black hole have extensive similarities [14]. However for a BI black hole in a cavity, there are some regions in the \tilde{Q} , \tilde{a} and \tilde{T} parameter space, where the global minimum of the free energy is at $x = 0$. Different phase structure from that of a BI-AdS black hole appears there. Our results imply that, in some region of the parameter space of the BI-AdS black hole, there might be other states of lower free energy with the same charge and temperature. Inspired by Schwarzschild-AdS black holes, one natural candidate is the thermal AdS space filled with charged particles. However, the backreaction of the charged particles on the AdS geometry should be considered, which could lead to formation of a naked singularity. It is inspiring to explore the possible equilibrium phases of lower free energy for charged AdS black holes.

Acknowledgments

We are grateful to Zheng Sun and Zhipeng Zhang for useful discussions and valuable comments. This work is supported in part by NSFC (Grant No. 11005016, 11175039 and 11375121).

Appendix A: Reduced Action

In this appendix, we use the reduced action method proposed in [12] to evaluate the Euclidean action of a NLED black hole in a cavity. Instead of employing ansatz functions to solve the equations of motion of the NLED-gravity system, we here start with the usual form of the static spherically symmetric metric and consider the reduced action for this specific metric first. In fact, the Euclidean continuation of the static spherically symmetric metric takes the form

$$ds^2 = b^2(r) d\tau^2 + \alpha^2(r) dr^2 + r^2 (d\theta^2 + \sin^2 \theta d\phi^2), \quad (\text{A1})$$

where b and α are free functions of r . We suppose that the Euclidean time is periodic with period 2π . In a canonical ensemble, the temperature T on the boundary of the cavity at

$r = r_B$ is fixed, which impose the boundary condition in terms of the reciprocal temperature:

$$\int b(r_B) d\tau = 2\pi b(r_B) = T^{-1}. \quad (\text{A2})$$

At the event horizon at $r = r_+$, one has $b(r_+) = 0$, and hence the $\tau - r$ part of the metric (A1) looks like a disc. To avoid a conical singularity at $r = r_+$, we require that

$$\alpha^{-1}(r_+) b'(r_+) = 1. \quad (\text{A3})$$

For the metric (A1), the Euclidean continuation of the action (1) becomes

$$\begin{aligned} \mathcal{S}^E = & -16\pi^2 \int_{r_+}^{r_B} dr \left\{ \left[\frac{1}{\alpha(r)} + \alpha(r) \right] b(r) + \frac{2rb'(r)}{\alpha(r)} \right\} + 32\pi^2 r_B b(r_B) \\ & - 16\pi^2 r_+^2 - 8\pi^2 \int_{r_+}^{r_B} dr r^2 a(r) b(r) \mathcal{L}(s, p). \end{aligned} \quad (\text{A4})$$

Varying the above action with respect to $\alpha(r)$ and $b(r)$ gives that

$$E_{\tau\tau} = \frac{1}{2}T_{\tau\tau} \text{ and } E_{rr} = \frac{1}{2}T_{rr}, \quad (\text{A5})$$

where $T_{\mu\nu}$, the energy-momentum tensor for the NLED field, is given by (6), and $E_{\mu\nu} = R_{\mu\nu} - \frac{1}{2}Rg_{\mu\nu}$ is the Einstein tensor. Note that E_τ^r and E_r^r are

$$E_\tau^r = \frac{1}{\alpha^2(r)r^2} - \frac{1}{r^2} - \frac{2\alpha'(r)}{\alpha^3(r)r} \text{ and } E_r^r = \frac{1}{\alpha^2(r)r^2} - \frac{1}{r^2} + \frac{2b'(r)}{rb(r)\alpha^2(r)}. \quad (\text{A6})$$

For the NLED field, we take the static spherical symmetry and gauge symmetry into account and assume that

$$A_\mu dx^\mu = A_\tau(r) d\tau. \quad (\text{A7})$$

For this ansatz, the equations of motion (A5) becomes

$$\frac{1}{\alpha^2 r^2} - \frac{1}{r^2} - \frac{2\alpha'}{\alpha^3 r} = \frac{1}{2} \left[\mathcal{L} \left(-\frac{\alpha^{-2} b^{-2}}{2} A_\tau'^2, 0 \right) + G^{r\tau} A_\tau' \right], \quad (\text{A8})$$

$$\frac{1}{\alpha^2 r^2} - \frac{1}{r^2} + \frac{2b'}{rb\alpha^2} = \frac{1}{2} \left[\mathcal{L} \left(-\frac{\alpha^{-2} b^{-2}}{2} A_\tau'^2, 0 \right) + G^{r\tau} A_\tau' \right], \quad (\text{A9})$$

where $G_{r\tau} = \mathcal{L}^{(1,0)} \left(-\frac{\alpha^{-2} b^{-2}}{2} A_\tau'^2, 0 \right) A_\tau'$. Moreover, varying the reduced action (A4) with respect to A_τ leads to

$$\partial_r (r^2 G^{r\tau}) = 0. \quad (\text{A10})$$

Subtracting eqns. (A8) from (A9), one finds that

$$\frac{\alpha'}{\alpha} = -\frac{b'}{b} \Rightarrow \alpha(r) = C b^{-1}(r), \quad (\text{A11})$$

where C is a constant. Actually, C can be determined by eqn. (A3):

$$C = -\frac{\alpha^3(r_+)}{\alpha'(r_+)}. \quad (\text{A12})$$

We can rescale $\tau \rightarrow C\tau$, and hence we have $b \rightarrow C^{-1}b = \alpha^{-1}$. So after this rescaling, the metric (A1) becomes

$$ds^2 = f(r) d\tau^2 + \frac{dr^2}{f(r)} + r^2 (d\theta^2 + \sin^2 \theta d\phi^2), \quad (\text{A13})$$

where we define $f(r) = \alpha^{-2}(r)$, and the period of τ is $2\pi C$.

Since A_τ and $G^{r\tau}$ is rescaled by $A_\tau \rightarrow C^{-1}A_\tau$ and $G^{r\tau} \rightarrow CG^{r\tau}$, respectively, eqns. (A8) and (A10) becomes

$$\frac{f(r)}{r^2} - \frac{1}{r^2} + \frac{f'(r)}{r} = \frac{1}{2} \left[\mathcal{L} \left(-\frac{A_\tau'^2(r)}{2}, 0 \right) + G^{r\tau} A_\tau'(r) \right], \quad (\text{A14})$$

$$\partial_r (r^2 G^{r\tau}) = 0, \quad (\text{A15})$$

which are just the Euclidean version of eqns. (8) and (10). Therefore, the solutions to the above equations are

$$\begin{aligned} f(r) &= 1 - \frac{r_+}{r} + \frac{1}{2r} \int_{r_+}^r dr r^2 \mathcal{L} \left(-\frac{A_\tau'^2(r)}{2}, 0 \right) - \frac{iQ}{2r} A_\tau(r), \\ G^{r\tau} &\equiv \mathcal{L}' \left(-\frac{A_\tau'^2(r)}{2}, 0 \right) A_\tau'(r) = -\frac{iQ}{r^2}, \end{aligned} \quad (\text{A16})$$

where Q is the charge of the black hole as discussed before. Plugging the solutions (A16) into the the Euclidean action (A4), we find that

$$\mathcal{S}^E = \frac{16\pi r_B}{T} \left[1 - \sqrt{f(r_B)} \right] - S, \quad (\text{A17})$$

where $S = 16\pi^2 r_+^2$ is the entropy of the black hole.

-
- [1] S. W. Hawking and D. N. Page, “Thermodynamics of Black Holes in anti-De Sitter Space,” Commun. Math. Phys. **87**, 577 (1983). doi:10.1007/BF01208266
- [2] J. M. Maldacena, “The Large N limit of superconformal field theories and supergravity,” Int. J. Theor. Phys. **38**, 1113 (1999) [Adv. Theor. Math. Phys. **2**, 231 (1998)] doi:10.1023/A:1026654312961, 10.4310/ATMP.1998.v2.n2.a1 [hep-th/9711200].

- [3] S. S. Gubser, I. R. Klebanov and A. M. Polyakov, “Gauge theory correlators from non-critical string theory,” *Phys. Lett. B* **428**, 105 (1998) doi:10.1016/S0370-2693(98)00377-3 [hep-th/9802109].
- [4] E. Witten, “Anti-de Sitter space and holography,” *Adv. Theor. Math. Phys.* **2**, 253 (1998) doi:10.4310/ATMP.1998.v2.n2.a2 [hep-th/9802150].
- [5] E. Witten, “Anti-de Sitter space, thermal phase transition, and confinement in gauge theories,” *Adv. Theor. Math. Phys.* **2**, 505 (1998) doi:10.4310/ATMP.1998.v2.n3.a3 [hep-th/9803131].
- [6] A. Chamblin, R. Emparan, C. V. Johnson and R. C. Myers, “Charged AdS black holes and catastrophic holography,” *Phys. Rev. D* **60**, 064018 (1999) doi:10.1103/PhysRevD.60.064018 [hep-th/9902170].
- [7] A. Chamblin, R. Emparan, C. V. Johnson and R. C. Myers, “Holography, thermodynamics and fluctuations of charged AdS black holes,” *Phys. Rev. D* **60**, 104026 (1999) doi:10.1103/PhysRevD.60.104026 [hep-th/9904197].
- [8] M. M. Caldarelli, G. Cognola and D. Klemm, “Thermodynamics of Kerr-Newman-AdS black holes and conformal field theories,” *Class. Quant. Grav.* **17**, 399 (2000) doi:10.1088/0264-9381/17/2/310 [hep-th/9908022].
- [9] R. G. Cai, “Gauss-Bonnet black holes in AdS spaces,” *Phys. Rev. D* **65**, 084014 (2002) doi:10.1103/PhysRevD.65.084014 [hep-th/0109133].
- [10] D. Kubiznak and R. B. Mann, “P-V criticality of charged AdS black holes,” *JHEP* **1207**, 033 (2012) doi:10.1007/JHEP07(2012)033 [arXiv:1205.0559 [hep-th]].
- [11] J. W. York, Jr., “Black hole thermodynamics and the Euclidean Einstein action,” *Phys. Rev. D* **33**, 2092 (1986). doi:10.1103/PhysRevD.33.2092
- [12] H. W. Braden, J. D. Brown, B. F. Whiting and J. W. York, Jr., “Charged black hole in a grand canonical ensemble,” *Phys. Rev. D* **42**, 3376 (1990). doi:10.1103/PhysRevD.42.3376
- [13] S. Carlip and S. Vaidya, “Phase transitions and critical behavior for charged black holes,” *Class. Quant. Grav.* **20**, 3827 (2003) doi:10.1088/0264-9381/20/16/319 [gr-qc/0306054].
- [14] A. P. Lundgren, “Charged black hole in a canonical ensemble,” *Phys. Rev. D* **77**, 044014 (2008) doi:10.1103/PhysRevD.77.044014 [gr-qc/0612119].
- [15] J. X. Lu, S. Roy and Z. Xiao, “Phase transitions and critical behavior of black branes in canonical ensemble,” *JHEP* **1101**, 133 (2011) doi:10.1007/JHEP01(2011)133 [arXiv:1010.2068 [hep-th]].

- [16] C. Wu, Z. Xiao and J. Xu, “Bubbles and Black Branes in Grand Canonical Ensemble,” *Phys. Rev. D* **85**, 044009 (2012) doi:10.1103/PhysRevD.85.044009 [arXiv:1108.1347 [hep-th]].
- [17] J. X. Lu, R. Wei and J. Xu, “The phase structure of black D1/D5 (F/NS5) system in canonical ensemble,” *JHEP* **1212**, 012 (2012) doi:10.1007/JHEP12(2012)012 [arXiv:1210.0708 [hep-th]].
- [18] J. X. Lu and R. Wei, “Modulating the phase structure of black D6 branes in canonical ensemble,” *JHEP* **1304**, 100 (2013) doi:10.1007/JHEP04(2013)100 [arXiv:1301.1780 [hep-th]].
- [19] D. Zhou and Z. Xiao, “Phase structures of the black Dp - $D(p+4)$ -brane system in various ensembles I: thermal stability,” *JHEP* **1507**, 134 (2015) doi:10.1007/JHEP07(2015)134 [arXiv:1502.00261 [hep-th]].
- [20] Z. Xiao and D. Zhou, “Phase structures of the black Dp - $D(p+4)$ -brane system in various ensembles II: electrical and thermodynamic stability,” *JHEP* **1509**, 028 (2015) doi:10.1007/JHEP09(2015)028 [arXiv:1507.02088 [hep-th]].
- [21] P. Basu, C. Krishnan and P. N. B. Subramanian, “Hairy Black Holes in a Box,” *JHEP* **1611**, 041 (2016) doi:10.1007/JHEP11(2016)041 [arXiv:1609.01208 [hep-th]].
- [22] Y. Peng, B. Wang and Y. Liu, “On the thermodynamics of the black hole and hairy black hole transitions in the asymptotically flat spacetime with a box,” *Eur. Phys. J. C* **78**, no. 3, 176 (2018) doi:10.1140/epjc/s10052-018-5652-0 [arXiv:1708.01411 [hep-th]].
- [23] Y. Peng, “Studies of a general flat space/boson star transition model in a box through a language similar to holographic superconductors,” *JHEP* **1707**, 042 (2017) doi:10.1007/JHEP07(2017)042 [arXiv:1705.08694 [hep-th]].
- [24] Y. Peng, “Scalar field configurations supported by charged compact reflecting stars in a curved spacetime,” *Phys. Lett. B* **780**, 144 (2018) doi:10.1016/j.physletb.2018.02.068 [arXiv:1801.02495 [gr-qc]].
- [25] N. Sanchis-Gual, J. C. Degollado, P. J. Montero, J. A. Font and C. Herdeiro, “Explosion and Final State of an Unstable Reissner-Nordstrom Black Hole,” *Phys. Rev. Lett.* **116**, no. 14, 141101 (2016) doi:10.1103/PhysRevLett.116.141101 [arXiv:1512.05358 [gr-qc]].
- [26] S. R. Dolan, S. Ponglertsakul and E. Winstanley, “Stability of black holes in Einstein-charged scalar field theory in a cavity,” *Phys. Rev. D* **92**, no. 12, 124047 (2015) doi:10.1103/PhysRevD.92.124047 [arXiv:1507.02156 [gr-qc]].
- [27] S. Ponglertsakul, E. Winstanley and S. R. Dolan, “Stability of gravitating charged-scalar solitons in a cavity,” *Phys. Rev. D* **94**, no. 2, 024031 (2016) doi:10.1103/PhysRevD.94.024031

- [arXiv:1604.01132 [gr-qc]].
- [28] N. Sanchis-Gual, J. C. Degollado, C. Herdeiro, J. A. Font and P. J. Montero, “Dynamical formation of a Reissner-Nordstrom black hole with scalar hair in a cavity,” *Phys. Rev. D* **94**, no. 4, 044061 (2016) doi:10.1103/PhysRevD.94.044061 [arXiv:1607.06304 [gr-qc]].
 - [29] S. Ponglertsakul and E. Winstanley, “Effect of scalar field mass on gravitating charged scalar solitons and black holes in a cavity,” *Phys. Lett. B* **764**, 87 (2017) doi:10.1016/j.physletb.2016.10.073 [arXiv:1610.00135 [gr-qc]].
 - [30] N. Sanchis-Gual, J. C. Degollado, J. A. Font, C. Herdeiro and E. Radu, “Dynamical formation of a hairy black hole in a cavity from the decay of unstable solitons,” *Class. Quant. Grav.* **34**, no. 16, 165001 (2017) doi:10.1088/1361-6382/aa7d1f [arXiv:1611.02441 [gr-qc]].
 - [31] O. J. C. Dias and R. Masachs, “Charged black hole bombs in a Minkowski cavity,” *Class. Quant. Grav.* **35**, no. 18, 184001 (2018) doi:10.1088/1361-6382/aad70b [arXiv:1801.10176 [gr-qc]].
 - [32] O. J. C. Dias and R. Masachs, “Evading no-hair theorems: hairy black holes in a Minkowski box,” *Phys. Rev. D* **97**, no. 12, 124030 (2018) doi:10.1103/PhysRevD.97.124030 [arXiv:1802.01603 [gr-qc]].
 - [33] L. McGough, M. Mezei and H. Verlinde, “Moving the CFT into the bulk with $T\bar{T}$,” *JHEP* **1804**, 010 (2018) doi:10.1007/JHEP04(2018)010 [arXiv:1611.03470 [hep-th]].
 - [34] H. H. Soleng, “Charged black points in general relativity coupled to the logarithmic U(1) gauge theory,” *Phys. Rev. D* **52**, 6178 (1995) doi:10.1103/PhysRevD.52.6178 [hep-th/9509033].
 - [35] H. Maeda, M. Hassaine and C. Martinez, “Lovelock black holes with a nonlinear Maxwell field,” *Phys. Rev. D* **79**, 044012 (2009) doi:10.1103/PhysRevD.79.044012 [arXiv:0812.2038 [gr-qc]].
 - [36] S. H. Hendi, B. Eslam Panah, S. Panahiyan and A. Sheykhi, “Dilatonic BTZ black holes with power-law field,” *Phys. Lett. B* **767**, 214 (2017) doi:10.1016/j.physletb.2017.01.066 [arXiv:1703.03403 [gr-qc]].
 - [37] J. Tao, P. Wang and H. Yang, “Testing holographic conjectures of complexity with Born-Infeld black holes,” *Eur. Phys. J. C* **77**, no. 12, 817 (2017) doi:10.1140/epjc/s10052-017-5395-3 [arXiv:1703.06297 [hep-th]].
 - [38] X. Guo, P. Wang and H. Yang, “Membrane Paradigm and Holographic DC Conductivity for Nonlinear Electrodynamics,” *Phys. Rev. D* **98**, no. 2, 026021 (2018)

- doi:10.1103/PhysRevD.98.026021 [arXiv:1711.03298 [hep-th]].
- [39] B. Mu, P. Wang and H. Yang, “Holographic DC Conductivity for a Power-law Maxwell Field,” *Eur. Phys. J. C* **78**, no. 12, 1005 (2018) doi:10.1140/epjc/s10052-018-6491-8 [arXiv:1711.06569 [hep-th]].
 - [40] S. H. Hendi and M. H. Vahidinia, “Extended phase space thermodynamics and P-V criticality of black holes with a nonlinear source,” *Phys. Rev. D* **88**, no. 8, 084045 (2013) doi:10.1103/PhysRevD.88.084045 [arXiv:1212.6128 [hep-th]].
 - [41] J. X. Mo, G. Q. Li and X. B. Xu, “Effects of power-law Maxwell field on the critical phenomena of higher dimensional dilaton black holes,” *Phys. Rev. D* **93**, no. 8, 084041 (2016) doi:10.1103/PhysRevD.93.084041 [arXiv:1601.05500 [gr-qc]].
 - [42] C. H. Nam, “Non-linear charged dS black hole and its thermodynamics and phase transitions,” *Eur. Phys. J. C* **78**, no. 5, 418 (2018). doi:10.1140/epjc/s10052-018-5922-x
 - [43] M. Dehghani, “Thermodynamic properties of dilaton black holes with nonlinear electrodynamics,” *Phys. Rev. D* **98**, no. 4, 044008 (2018). doi:10.1103/PhysRevD.98.044008
 - [44] E. Ayon-Beato and A. Garcia, “Regular black hole in general relativity coupled to nonlinear electrodynamics,” *Phys. Rev. Lett.* **80**, 5056 (1998) doi:10.1103/PhysRevLett.80.5056 [gr-qc/9911046].
 - [45] E. Ayon-Beato and A. Garcia, “New regular black hole solution from nonlinear electrodynamics,” *Phys. Lett. B* **464**, 25 (1999) doi:10.1016/S0370-2693(99)01038-2 [hep-th/9911174].
 - [46] K. A. Bronnikov, “Regular magnetic black holes and monopoles from nonlinear electrodynamics,” *Phys. Rev. D* **63**, 044005 (2001) doi:10.1103/PhysRevD.63.044005 [gr-qc/0006014].
 - [47] M. Born and L. Infeld, “Foundations of the new field theory,” *Proc. Roy. Soc. Lond. A* **144**, 425 (1934). doi:10.1098/rspa.1934.0059
 - [48] T. K. Dey, “Born-Infeld black holes in the presence of a cosmological constant,” *Phys. Lett. B* **595**, 484 (2004) doi:10.1016/j.physletb.2004.06.047 [hep-th/0406169].
 - [49] R. G. Cai, D. W. Pang and A. Wang, “Born-Infeld black holes in (A)dS spaces,” *Phys. Rev. D* **70**, 124034 (2004) doi:10.1103/PhysRevD.70.124034 [hep-th/0410158].
 - [50] S. Fernando and D. Krug, “Charged black hole solutions in Einstein-Born-Infeld gravity with a cosmological constant,” *Gen. Rel. Grav.* **35**, 129 (2003) doi:10.1023/A:1021315214180 [hep-th/0306120].
 - [51] S. Fernando, “Thermodynamics of Born-Infeld-anti-de Sitter black holes in the grand

- canonical ensemble,” *Phys. Rev. D* **74**, 104032 (2006) doi:10.1103/PhysRevD.74.104032 [hep-th/0608040].
- [52] R. Banerjee, S. Ghosh and D. Roychowdhury, “New type of phase transition in Reissner Nordstrom–AdS black hole and its thermodynamic geometry,” *Phys. Lett. B* **696**, 156 (2011) doi:10.1016/j.physletb.2010.12.010 [arXiv:1008.2644 [gr-qc]].
- [53] R. Banerjee and D. Roychowdhury, “Critical phenomena in Born-Infeld AdS black holes,” *Phys. Rev. D* **85**, 044040 (2012) doi:10.1103/PhysRevD.85.044040 [arXiv:1111.0147 [gr-qc]].
- [54] A. Lala and D. Roychowdhury, “Ehrenfest’s scheme and thermodynamic geometry in Born-Infeld AdS black holes,” *Phys. Rev. D* **86**, 084027 (2012) doi:10.1103/PhysRevD.86.084027 [arXiv:1111.5991 [gr-qc]].
- [55] R. Banerjee and D. Roychowdhury, “Critical behavior of Born Infeld AdS black holes in higher dimensions,” *Phys. Rev. D* **85**, 104043 (2012) doi:10.1103/PhysRevD.85.104043 [arXiv:1203.0118 [gr-qc]].
- [56] M. Azreg-Ainou, “Black hole thermodynamics: No inconsistency via the inclusion of the missing $P - V$ terms,” *Phys. Rev. D* **91**, 064049 (2015) doi:10.1103/PhysRevD.91.064049 [arXiv:1411.2386 [gr-qc]].
- [57] S. H. Hendi, B. Eslam Panah and S. Panahiyan, “Einstein-Born-Infeld-Massive Gravity: adS-Black Hole Solutions and their Thermodynamical properties,” *JHEP* **1511**, 157 (2015) doi:10.1007/JHEP11(2015)157 [arXiv:1508.01311 [hep-th]].
- [58] M. Kord Zangeneh, A. Dehyadegari, M. R. Mehdizadeh, B. Wang and A. Sheykhi, “Thermodynamics, phase transitions and Ruppeiner geometry for Einstein–dilaton–Lifshitz black holes in the presence of Maxwell and Born–Infeld electrodynamics,” *Eur. Phys. J. C* **77**, no. 6, 423 (2017) doi:10.1140/epjc/s10052-017-4989-0 [arXiv:1610.06352 [hep-th]].
- [59] X. X. Zeng, X. M. Liu and L. F. Li, “Phase structure of the Born–Infeld–anti-de Sitter black holes probed by non-local observables,” *Eur. Phys. J. C* **76**, no. 11, 616 (2016) doi:10.1140/epjc/s10052-016-4463-4 [arXiv:1601.01160 [hep-th]].
- [60] S. Li, H. Lu and H. Wei, “Dyonic (A)dS Black Holes in Einstein-Born-Infeld Theory in Diverse Dimensions,” *JHEP* **1607**, 004 (2016) doi:10.1007/JHEP07(2016)004 [arXiv:1606.02733 [hep-th]].
- [61] D. C. Zou, S. J. Zhang and B. Wang, “Critical behavior of Born-Infeld AdS black holes in the extended phase space thermodynamics,” *Phys. Rev. D* **89**, no. 4, 044002 (2014)

- doi:10.1103/PhysRevD.89.044002 [arXiv:1311.7299 [hep-th]].
- [62] S. Hossein Hendi, B. Eslam Panah, S. Panahiyan and M. Hassaine, “BTZ dilatonic black holes coupled to Maxwell and Born-Infeld electrodynamics,” *Phys. Rev. D* **98**, no. 8, 084006 (2018) doi:10.1103/PhysRevD.98.084006 [arXiv:1712.04328 [physics.gen-ph]].
 - [63] S. Gunasekaran, R. B. Mann and D. Kubiznak, “Extended phase space thermodynamics for charged and rotating black holes and Born-Infeld vacuum polarization,” *JHEP* **1211**, 110 (2012) doi:10.1007/JHEP11(2012)110 [arXiv:1208.6251 [hep-th]].
 - [64] A. Dehyadegari and A. Sheykhi, “Reentrant phase transition of Born-Infeld-AdS black holes,” *Phys. Rev. D* **98**, no. 2, 024011 (2018) doi:10.1103/PhysRevD.98.024011 [arXiv:1711.01151 [gr-qc]].
 - [65] P. Wang, H. Wu and H. Yang, “Thermodynamics and Phase Transitions of Nonlinear Electrodynamics Black Holes in an Extended Phase Space,” arXiv:1808.04506 [gr-qc].
 - [66] R. Pellicer and R. J. Torrence, “Nonlinear electrodynamics and general relativity,” *J. Math. Phys.* **10**, 1718 (1969). doi:10.1063/1.1665019
 - [67] J. Plebanski, “Non-Linear Electrodynamics. A Study” (Monograph of CINVESTAV, Mexico City, 1966).
 - [68] V. Balasubramanian and P. Kraus, “A Stress tensor for Anti-de Sitter gravity,” *Commun. Math. Phys.* **208**, 413 (1999) doi:10.1007/s002200050764 [hep-th/9902121].
 - [69] R. Emparan, C. V. Johnson and R. C. Myers, “Surface terms as counterterms in the AdS / CFT correspondence,” *Phys. Rev. D* **60**, 104001 (1999) doi:10.1103/PhysRevD.60.104001 [hep-th/9903238].